ORIGINAL RESEARCH

Recombinant Interleukin-19 Suppresses the Formation and Progression of Experimental Abdominal Aortic Aneurysms

Hiroki Tanaka, MD, PhD;Baohui Xu iD, MD, PhD;Haojun Xuan, MD; Yingbin Ge iD, MD, PhD; Yan Wang, PhD; Yankui Li iD, MD, PhD; Wei Wang iD, MD, PhD; Jia Guo, MD, PhD; Sihai Zhao, MD, PhD; Keith J. Glover, MD; Xiaoya Zheng, MD, PhD; Shuai Liu, MD; Kazunori Inuzuka, MD; Naoki Fujimura, MD, PhD; Yuko Furusho iD, MD, PhD; Toru Ikezoe, MD; Takahiro Shoji iD, MD; Lixin Wang, MD, PhD; Weiguo Fu, MD, PhD; Jianhua Huang, MD; Naoki Unno, MD, PhD; Ronald L. Dalman, MD

BACKGROUND: Interleukin-19 is an immunosuppressive cytokine produced by immune and nonimmune cells, but its role in abdominal aortic aneurysm (AAA) pathogenesis is not known. This study aimed to investigate interleukin-19 expression in, and influences on, the formation and progression of experimental AAAs.

METHODS AND RESULTS: Human specimens were obtained at aneurysm repair surgery or from transplant donors. Experimental AAAs were created in 10- to 12-week-old male mice via intra-aortic elastase infusion. Influence and potential mechanisms of interleukin-19 treatment on AAAs were assessed via ultrasonography, histopathology, flow cytometry, and gene expression profiling. Immunohistochemistry revealed augmented interleukin-19 expression in both human and experimental AAAs. In mice, interleukin-19 treatment before AAA initiation via elastase infusion suppressed aneurysm formation and progression, with attenuation of medial elastin degradation, smooth-muscle depletion, leukocyte infiltration, neoangiogenesis, and matrix metalloproteinase 2 and 9 expression. Initiation of interleukin-19 treatment after AAA creation limited further aneurysmal degeneration. In additional experiments, interleukin-19 treatment inhibited murine macrophage recruitment following intraperitoneal thioglycolate injection. In classically or alternatively activated macrophages in vitro, interleukin-19 downregulated mRNA expression of inducible nitric oxide synthase, chemokine C-C motif ligand 2, and metalloproteinases 2 and 9 without apparent effect on cytokine-expressing helper or cytotoxic T-cell differentiation, nor regulatory T cellularity, in the aneurysmal aorta or spleen of interleukin-19–treated mice. Interleukin-19 also suppressed AAAs created via angiotensin II infusion in hyperlipidemic mice.

CONCLUSIONS: Based on human evidence and experimental modeling observations, interleukin-19 may influence the development and progression of AAAs.

Key Words: abdominal aortic aneurysm ■ angiogenesis ■ cytokines ■ interleukin-19 ■ macrophages

Abdominal aortic aneurysm (AAA) is a common, age-related degenerative disease of the infrarenal aortic segment. Characteristic histopathologic features of advanced AAA disease include medial elastin and vascular smooth-muscle cell (SMC) depletion, transmural inflammatory cell accumulation, and neoangiogenesis. Multiple lines of evidence suggest that inflammation is central to the initiation and progression of AAAs,[1] including a recent prospective study showing the positive association of aortic uptake

CLINICAL PERSPECTIVE

What Is New?

- Recombinant cytokine interleukin-19 suppressed the formation and progression of experimental abdominal aortic aneurysms in 2 distinct and complementary mouse abdominal aortic aneurysm modeling systems.
- Abdominal aortic aneurysm suppression by interleukin-19 was associated with attenuation of medial elastin and smooth-muscle destruction, mural leukocyte infiltration and neoangiogenesis, matrix metalloproteinases, and chemokine C-C motif ligand 2.

What Are the Clinical Implications?

- Medical interventions based on recombinant interleukin-19 or its derivative strategies may hold the translational relevance for clinical abdominal aortic aneurysm disease management.

Nonstandard Abbreviations and Acronyms

AAA	abdominal aortic aneurysm
BMDM	bone marrow–derived macrophage
CCL	chemokine (C-C motif) ligand
Foxp3	Forkhead Box P3
MMP	matrix metalloproteinase
PPE	porcine pancreatic elastase
rIL	recombinant interleukin
SMC	smooth-muscle cell
TGF	transforming growth factor
Treg	regulatory T cell

of ultrasmall superparamagnetic iron oxide particles with AAA enlargement, the risk for surgical aneurysm repair, and aneurysm-specific mortality.[2]

Cytokines are biologically active small peptides, recognized by their cognate receptors on targeting cells, and involved in triggering, sustaining, and resolving inflammatory responses. Proinflammatory cytokines such as interleukins-1β, -6, -8, and -17, as well as interferon-γ; tumor necrosis factor-α; and chemokine (C-C motif) ligand (CCL) 2, CCL5, and chemokine (C-X-C motif) ligand 12 all promote experimental AAA pathogenesis.[3–13] In contrast, the role of anti-inflammatory cytokine involvement, except for the well-studied transforming growth factor-beta (TGF-β) specifically,[14–18] is less well understood.

Interleukin-19 is an interleukin-10 family cytokine produced by immune (monocytes/macrophages,

B and T) and vascular structural (endothelial and smooth-muscle) cells.[19] Distinct from interleukin-10, which activates the interleukin-10RA/interleukin-10RB heterodimer receptor to upregulate anti-inflammatory responses in target cells, interleukin-19 uses interleukin-20RA/IL-20RB heterodimer receptor to affect pro- or anti-inflammatory responses in target cells on the basis of pathophysiological conditions.[19] In prior studies, exogenous interleukin-19 administration attenuated experimental atherosclerosis, neointimal hyperplasia, ischemic myocardial infarction, and central nervous system injury.[19–24] Although many mediators present in the aneurysmal aorta are capable of inducing interleukin-19 expression,[25] the specific effect of interleukin-19 on AAA formation and progression remains unknown.

The present study evaluated the expression of interleukin-19 in clinical and experimental AAAs, as well as the influence of recombinant interleukin-19 (rIL-19) treatment on experimental AAA formation and progression in 2 mechanistically distinct but complementary murine models.

METHODS

Data and Method Availability

The authors declare that all data and methods are available within the article and its online supplementary files.

Mice

Wild-type C57BL/6J and apolipoprotein E knockout mice on BALB/c genetic background were purchased from the Jackson Laboratory (Bar Harbor, ME), or Japan SLC Inc. (Hamamatsu, Shizuoka, Japan) (Table S1). Because AAA is a male-dominant disease with significant sex-based differences in phenotypic expression and natural history, only single-sex (male) mice at 10 to 12 weeks of age were used. BALB/C background mice were the only apolipoprotein E–deficient strain available in Hamamatsu University, Japan, where the experiments on angiotensin II–induced AAAs were conducted. Experimental procedures and care for laboratory animals were performed in compliance with the Stanford University and Hamamatsu University School of Medicine Laboratory Animal Care Guidelines, with research protocols approved by their respective review committees.

AAA Creation

Experimental AAAs were created via transient porcine pancreatic elastase (PPE) infusion into a controlled segment of the infrarenal aorta in wild-type C57BL/6J mice as previously described.[10,26–28] All surgical procedures, including laparotomy, ligation of aortic branches

and infrarenal segment, aortotomy, PPE infusion, and closure of aortotomy and laparotomy, were performed under inhaled anesthesia containing 2% isoflurane, sterile conditions, and a surgical microscope. Thirty microliters of PPE (type I, 1.5 units/mL in PBS, Table S1) were infused into a temporarily ligated infrarenal aortic segment for 5 minutes via a heat-tapered P-10 tubing.

In confirmatory experiments, additional AAAs were created in hyperlipidemic apolipoprotein E knockout mice on BALB/c genetic background by a 28-day subcutaneous infusion of human recombinant angiotensin II (angiotensin II, 1000 ng/min per kg) via an Alzet Model 2004 mini-osmotic minipump (Durect Corp, Cupertino, CA)[10,26,29] (Table S1). In both PPE and angiotensin II/apolipoprotein E knockout models, mice were housed in separated cages with free access to chow and water after surgical recovery.

Immunostaining and Quantification of Interleukin-19 in Aneurysmal Aorta

Aneurysmal and nonaneurysmal infrarenal abdominal aortic surgical specimens were obtained from patients undergoing open aneurysm repair surgery (n=19) and organ transplantation donors (n=8), respectively, at Central South University Xiangya Hospital (Changsha, China) and Fudan University Zhongshan Hospital (Shanghai, China). Collection and use of patient samples for this purpose has received prior approval by their respective institutional Human Subject Research Committees, with informed consent obtained from donors or their agents. Demographic details of the AAA patients are outlined in Table S2. Organ donors included 7 men and 1 woman, aged 41–60 years, with causes of death including motor vehicle crashes (n=3), cerebral hemorrhage (n=4), or complications arising from cerebral palsy (n=1).

For experimental AAAs, infrarenal aortas were harvested 14 days following PPE (aneurysmal) or PBS (nonaneurysmal) infusion. Human and mouse infrarenal aortas were fixed with 10% neutral formalin immediately following harvest, embedded in paraffin, and sectioned. For human specimens, intraluminal thrombus, if present, was removed before sectioning, and only aneurysmal aortic segments were used for analysis.

Aortic sections were stained with a rabbit anti–interleukin-19 antibody or concentration-matched normal rabbit IgG as the negative control using a standard biotin-streptavidin-peroxidase procedure following antigen retrial as previously described[30] (Table S1). For patient aortic specimens, 3 sections separated by 50 µm were strained and visualized using a peroxidase substrate (3,3′-diaminobenzidine) kit. One hundred cells in 5 randomly selected fields at 400-fold magnification were evaluated. Cells were considered as positively stained when the stained area exceeded 10% of the cytoplasm as evaluated using ImageJ software (http://imagej.nih/gov/ij, Version 1.49A, National Institutes of Health, Bethesda, MD). Interleukin-19 staining intensity was further graded as 0 (not detectable), 1 (weak but detectable staining above the background level), 2 (moderate staining), or 3 (intense staining).

Interleukin-19 Treatment

Mouse rIL-19 was daily administered intraperitoneally at a dose 10 µg/kg of starting 1 day before PPE infusion and continued for 14 days, or angiotensin II infusion and continued for 28 days, to determine the effect of rIL-19 supplementation on aneurysm initiation and progression in each model (Table S1).[31] In a subsequent experiment, rIL-19 was administered 4 days following PPE infusion and continued for 10 days to determine its effect on progression of established AAAs. In all experiments, equal volumes of PBS were administered to PPE-infused C57BL/6J mice or angiotensin II–infused apolipoprotein E knockout mice as corresponding vehicle controls for each cohort.

Measurements of Abdominal Aortic Diameters via Ultrasonography

Aneurysm formation and progression were imaged via serial measurements of infrarenal (PPE model) or suprarenal (angiotensin II/apolipoprotein E knockout model) aortic diameters using noninvasive transabdominal ultrasonography (40 MHz, Model Vevo 770, Visualsonics, Toronto, ON, Canada) as previously described.[26,27] Measurements were performed on days 0, 3, 7, and 14 for the PPE model, and days 0, 3, 7, 14, 21, and 28 for the angiotensin II/apolipoprotein E knockout model. AAAs were defined as present when the aorta experienced a ≥50% diameter increase over the baseline level, an aortic dissection was noted to be present (angiotensin II/apolipoprotein E knockout model only), or the mouse experienced death attributable to aneurysm rupture.

Histologic Assessments of Experimental AAAs

Mice were sacrificed 14 days following PPE infusion. Aortas were harvested, frozen-embedded in optimal cutting temperature media, sectioned (6 µm thickness), and acetone fixed. A standard biotin-streptavidin-peroxidase procedure was applied to stain macrophages (CD68), T cells (CD3), B cells (B220), regulatory T cells (Tregs) (Forkhead Box P3 [Foxp3]), neovessels (CD31), SMCs (SMC α actin), matrix metalloproteinase (MMP)2, MMP9, and CCL2, as previously described.[27] Medial elastin was stained using the Elastica Van Gieson staining procedure.[27]

Each histologic stain was performed in 3 inconsecutive aortic sections, each 50 μm apart, for individual mice. Sources, clone or catalog number, and working concentrations for primary antibodies, secondary antibodies, streptavidin-peroxidase conjugates, and other reagents are provided in Table S1.

For semiquantitative histology, the severity of medial elastin degradation and SMC depletion were graded as I (mild) to IV (severe) on Elastica Van Gieson- or SMC α actin antibody–stained sections, respectively, as described previously.[28] Individual leukocyte subsets and mural capillary density (also known as neoangiogenesis) were quantified as positively stained subsets of leukocytes, and CD31-positive vessels per aortic cross section, respectively.[27] Aortic expression of MMP 2, MMP 9, and CCL2 proteins were quantified as the percentage of positively stained area to total aortic cross-section area using ImageJ software.

Flow Cytometric Analysis of Cytokine-Producing T Cells and Tregs

Splenic lymphocytes were isolated from mice 14 days following PPE infusion and activated with phorbol 12-myristate 13-acetate and ionomycin for 4 hours as described previously.[28,30] Cells were then sequentially stained with monoclonal antibodies to CD4 and CD8, fixed and permeabilized, incubated with monoclonal antibodies to interleukin-10, interleukin-17, interferon-γ, and Foxp3, and analyzed on a flow cytometer (Table S1). Data were presented as the percentage of individual cytokine-producing cells in CD4$^+$ or CD8$^+$ T cells or the percentage of Foxp3-positive cells in CD4$^+$ T cells.

Evaluation of Bone Marrow–Derived Macrophage Activation Status

This evaluation was conducted as described previously.[27] Briefly, whole bone marrow cells from 10 weeks old male C57BL/6J mice were differentiated with macrophage colony-stimulating factor (20 ng/mL) for 1 week. As proposed by international experimental guidelines on macrophage polarization experiments,[32] resulting bone marrow–derived macrophages (BMDMs) were classically activated with lipopolysaccharides (20 ng/mL) (M or M1 macrophages) or alternatively activated with interleukin-4 (20 ng/mL) (M or M2 macrophages), in the presence or absence of rIL-19. Forty-eight hours thereafter, BMDMs were harvested, and total RNA was extracted for real-time quantitative reverse transcription polymerase chain reaction analysis using gene-specific primer sets (Table S3), including genes for inducible nitric oxide synthase (M1 macrophage marker), CCL2, IL-1β, MMP2 and MMP9 (proaneurysmal mediators) and TGF-β1 (M2 marker and antianeurysmal mediator). mRNA levels in M lipopolysaccharide macrophages and M interleukin-4 cells were presented as fold changes relative to BMDMs with vehicle treatment. The influence of interleukin-19 on the mRNA expression levels in M lipopolysaccharide macrophages and M interleukin-4 cells was expressed as the percentage of that for (M lipopolysaccharide macrophages or M interleukin-4) cells with vehicle treatment.

Thioglycolate-Induced Macrophage Recruitment

Male C57BL/6J mice at 8 weeks of age were administered 1 mL of sterilized 3% Brewer thioglycolate medium (Difco Laboratories, Detroit, MI) intraperitoneally. rIL-19 (10 μg/kg) or an equal volume of PBS as vehicle control was administered daily starting immediately before thioglycolate injection. Four days after thioglycolate injection, peritoneal macrophages were collected and stained with monoclonal antibodies against CD11b, CD115, and F4/80 followed by flow cytometric analysis (Table S1). Similar analyses were performed to quantify inflammatory monocytes and neutrophils in peripheral blood based on the expression of CD11b, Ly-6C, and Ly-6G antigens, as previously described.[33]

Statistical Analysis

All continuous variables are presented as mean±SE. One- or 2-way repeated measures ANOVA, Student's t test, or nonparametric Mann-Whitney tests were used to determine statistical difference for normally and nonnormally distributed data, respectively, between groups. The log-rank test was used to test the difference in cumulative aneurysm incidence and mortality between groups. In all statistical analyses, $P<0.05$ was considered significant. All statistical analyses were performed using Prism, version 6.0h (GraphPad Software, Inc, San Diego, CA). Statistical power and sample size calculations for similar experimental protocols have been detailed previously.[27]

RESULTS

Interleukin-19 Expression Is Increased in Clinical and Experimental Aneurysmal Aortas

On immunohistochemical analysis, abundant interleukin-19 staining was observed in experimental and clinical aneurysmal aortas compared with their respective controls (Figure 1). Normal rabbit IgG, the negative control for interleukin-19 antibody, stained neither human (Figure 1) nor mouse (not shown) AAA. These patterns support the conclusion that mural interleukin-19 expression is increased in clinical and experimental aneurysmal aortas.
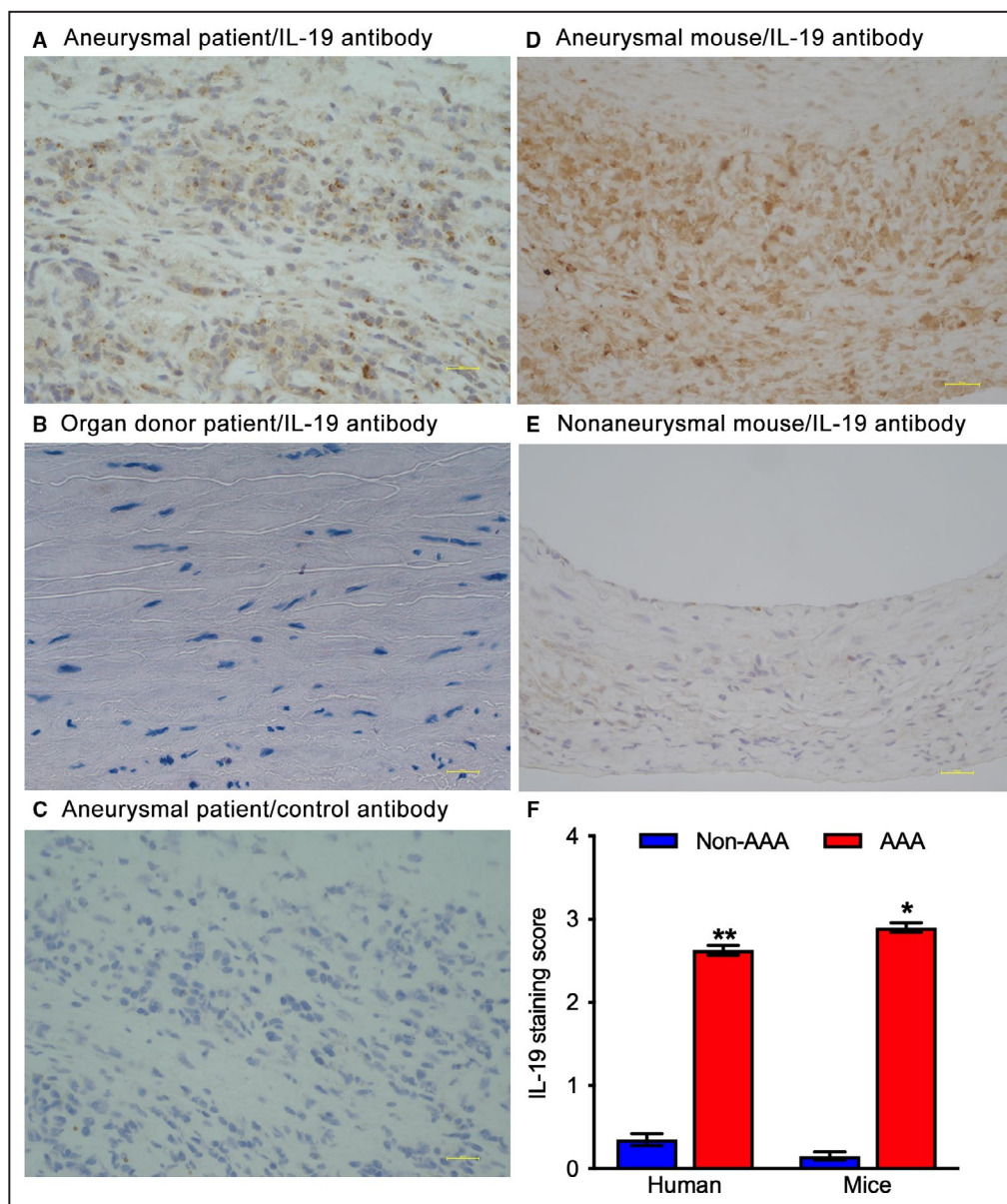
Figure 1. Expression of interleukin (IL)-19 in clinical and experimental aneurysmal aortas.
Immunohistochemical staining was performed on paraffin sections of aneurysmal patient aorta, nonaneurysmal organ donor patient and male mouse aortas, in the latter case 2 weeks after porcine pancreatic elastase (PPE, aneurysm) or PBS (nonaneurysm) infusion using an anti–IL-19 polyclonal or control antibody. **A**, **B**, **C**, Representative immunostaining images for IL-19 expression in human aneurysmal (**A**) and nonaneurysmal (**B**) aortas. No staining demonstrated in control antibody-stained aneurysmal aorta (**C**) and nonaneurysmal aorta (images not shown). **D** and **E**, IL-19 staining in aneurysmal (**D**) and nonaneurysmal (**E**) mouse aorta. No staining was noted in either aneurysmal or non-aneurysmal aorta for using control antibody (data not shown). **F**, Mean and standard error of IL-19 staining score in clinical (n=19) and experimental (n=4) aneurysmal and nonaneurysmal aortas (n=8 and 4 for organ donors and mice, respectively). Nonparametric Mann-Whitney test, *$P<0.05$ & **$P<0.01$ compared with PBS infusion and organ donors, respectively.

rIL-19 Attenuates Formation and Progression of Experimental AAAs

To determine the potential for interleukin-19 to modulate AAA pathogenesis, rIL-19 or vehicle (PBS) alone were given to mice starting 1 day before PPE infusion for 14 days. Relative body weight (percentage of the baseline level) was slightly but significantly reduced in interleukin-19 (93±3%) as compared with vehicle (106±5%) treated mice after 14 days. In vehicle-treated mice, aortic diameters enlarged progressively from day 3 through

days 7 to 14 following PPE infusion (Figures 2A and 2B). In contrast, rIL-19 administration markedly diminished aortic enlargement (Figures 2A and 2B). Average aortic diameters were significantly smaller in rIL-19–treated mice at all time points following PPE infusion (Figure 2B). AAAs formed in all vehicle-treated (5/5) and 56%% of rIL-19–treated mice (5/9), respectively, within 14 days following PPE infusion (Figure 2C). Elastica Van Gieson and anti-SMC α actin staining confirmed reduced medial elastin fragmentation and SMC loss in rIL-19–treated mice (Figures 2D and 2E). Together, these

results indicate that rIL-19 supplementation suppresses experimental aneurysm formation and progression.

rIL-19 Reduces Mural Leukocyte Accumulation and Neoangiogenesis

Because of the important role of leukocytes in AAA pathogenesis, we examined the influence of rIL-19 administration on characteristic mural leukocyte subsets in experimental aneurysms. CD68+ macrophages represented the majority of infiltrated leukocytes, with
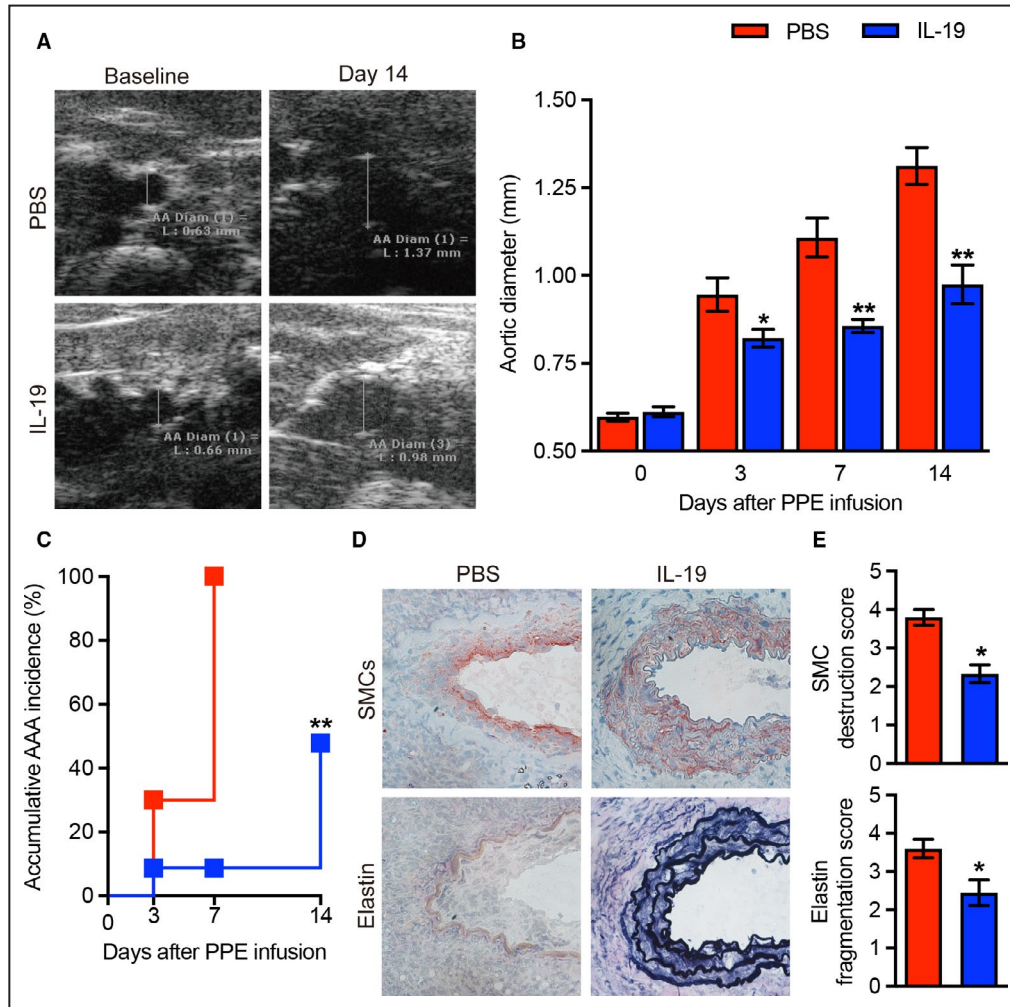

Figure 2. Recombinant interleukin (rIL)-19 suppresses the formation and progression of experimental abdominal aortic aneurysms (AAAs).
Male C57BL/6 mice were administered rIL-19 (10 ng/g per day, n=9), or an equal volume of phosphate-buffered saline (PBS) (n=5), starting 1 day before porcine pancreatic elastase (PPE) infusion for 14 days. AAAs were assessed by measuring maximal infrarenal aortic diameter via noninvasive ultrasonography. **A**, Representative aortic ultrasound images prior to (baseline), and 14 days following, PPE infusion. **B**, Serially measured aortic diameters (mean and standard error). Repeated measures 2-way analysis of variance (ANOVA) followed by 2 sample comparison test, *$P<0.05$ and **$P<0.01$ compared with PBS treatment at same time point. **C**, Cumulative AAA incidence. AAA: a ≥50% increase in the aortic diameter over the baseline level. The log-rank test, **$P<0.01$ compared with PBS treatment. **D**, Aortic histological images for medial elastin content (Elastica Van Gieson stain) and smooth-muscle cell [SMC] α actin) staining from same mouse in each group. **E**, Quantitative histologic scores (mean and standard error) of SMC destruction (upper) and medial elastin fragmentation (lower). Nonparametric Mann-Whitney test, *$P<0.05$ compared with PBS treatment. AA Diam indicates abdominal aortic diameter.

moderate accumulation of CD3^{+} T cells and B220^{+} B cells, in vehicle-treated aneurysmal aortas (Figure 3A), concentrated mostly in the adventitial region. rIL-19 treatment significantly attenuated aortic accumulation of all 3 leukocyte subsets (Figure 3B). Mural neovascularization, another hallmark of aneurysmal pathology, was also significantly attenuated (Figures 3A and 3B). Thus, rIL-19 was associated with reduced mural leukocyte infiltration and angiogenesis in treated mice.

rIL-19 Reduces CCL2, MMP2, and MMP9 Protein Expression

The chemokine CCL2 recruits circulating inflammatory monocytes to the aneurysmal aorta, where they differentiate into macrophages capable of producing extracellular matrix–degrading proteinases such as MMP2 and MMP9. The influence of rIL-19 administration on aortic CCL2 and MMP expression was assessed using semiquantitative immunohistochemistry. As demonstrated in Figure 4, CCL2 staining was remarkably attenuated by rIL-19 administration. Similarly, expression of both MMP proteins were also dramatically reduced. Thus, aortic monocyte chemotactic signal and extracellular matrix-degrading proteinase expression were reduced in rIL-19–treated AAA mice.

rIL-19 Attenuates Thioglycolate-Elicited Peritoneal Macrophage Accumulation

rIL-19 was administered immediately after thioglycolate injection to analyze its effects on macrophage
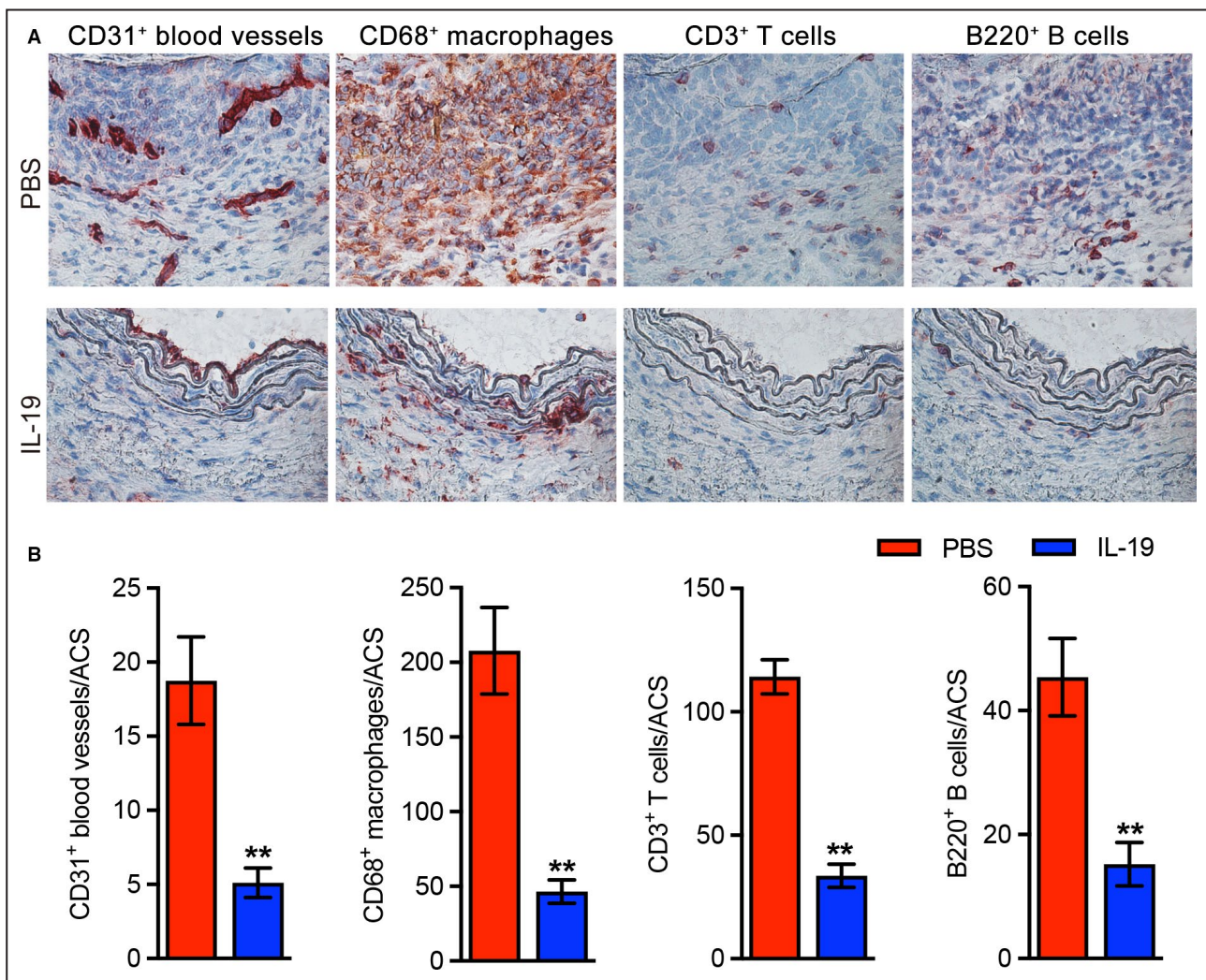
Figure 3. Recombinant interleukin (rIL)-19 attenuates mural leukocyte infiltration and angiogenesis.
Acetone-fixed aortic frozen sections were prepared from mice 14 days after porcine pancreatic elastase (PPE) infusion and stained with antibodies against CD31 for blood vessels/angiogenesis, CD68 for macrophages, CD3 for T cells and B220 for B cells, and quantified. **A**, Representative aortic histology for mural macrophages, T cells, B cells and angiogenesis. **B**, Quantification of mural macrophages, T cells, B cells, and angiogenesis. Results are presented as the mean and standard error of the numbers of macrophages, T cells, B cells, and neovessels per aortic cross section (ACS). Nonparametric Mann-Whitney test, **P<0.01 compared with PBS treatment. n=5-9 mice/group.

Figure 4. Recombinant interleukin (rIL)-19 attenuates expression of aortic matrix metalloproteinases (MMP) and C-C motif chemokine ligand 2 (CCL2).

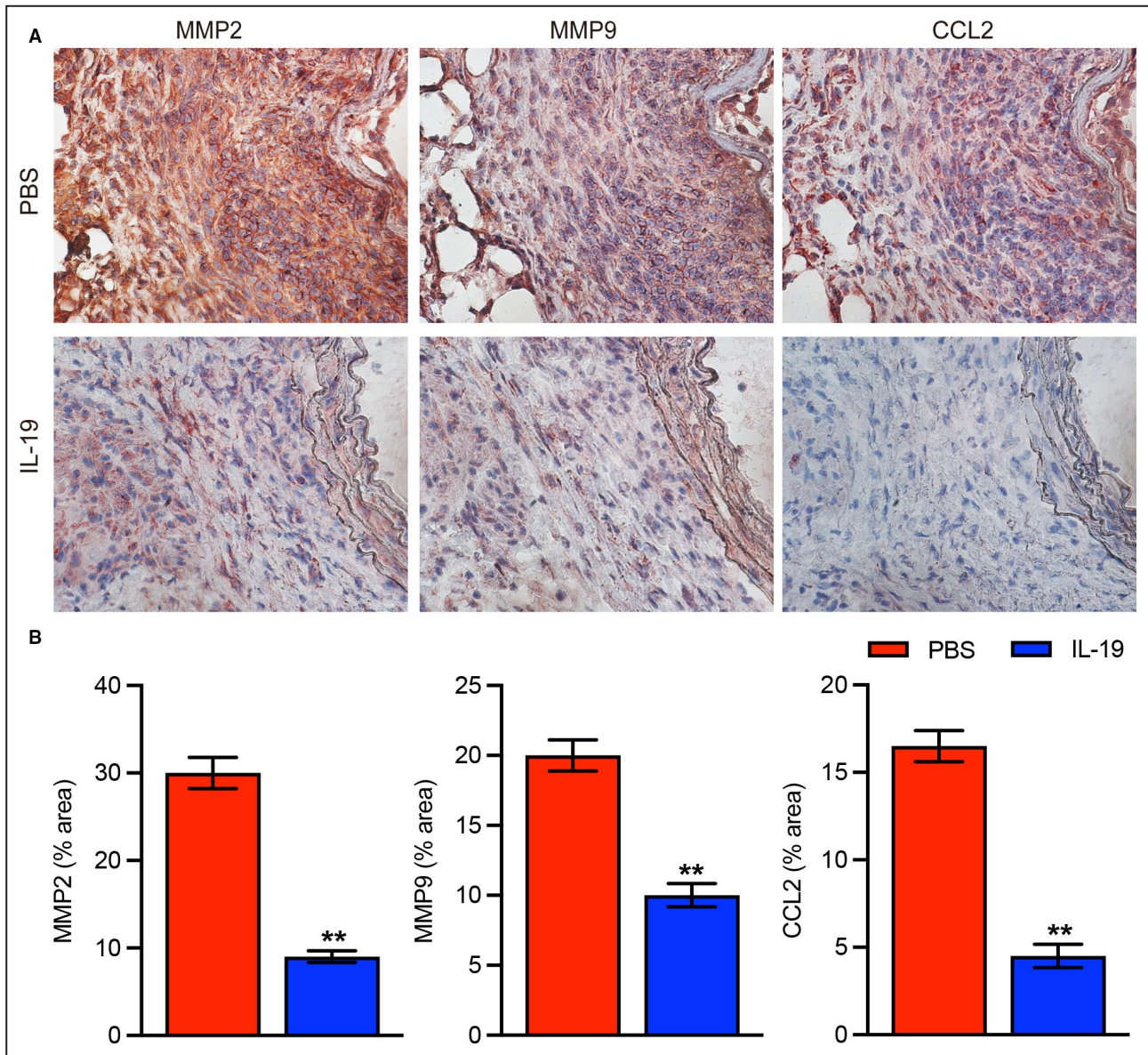Aortic frozen sections were prepared from mice 14 days following PPE infusion, and stained with a polyclonal antibody against MMP-2, MMP-9 or CCL-2. Staining data were quantified as the percentage of positively stained area in total area of aortic cross section. **A**, Representative histology for MMP2, MMP9 and CCL2. **B**, Quantification of MMP2, MMP9, and CCL2 staining (mean and standard error). Nonparametric Mann-Whitney test, **$P<0.01$ compared with PBS treatment. n=5-9 mice/group.

recruitment and circulating monocytes and neutrophils (Figure 5). rIL-19 administration resulted in a 32% decrease and 200% increase in the relative number of CD11b^highCD115^highF4/80^high and CD11b^highCD115^lowF4/80^high peritoneal macrophages, respectively. There were also significantly decreased and increased absolute numbers of CD11b^highCD115^highF4/80^high and CD11b^highCD115^lowF4/80^high macrophages, respectively, following rIL-19 treatment.

Consistent with reduced peritoneal macrophage recruitment, rIL-19 did increase the relative and absolute numbers of circulating inflammatory monocytes,

as defined as CD11b^+Ly6-C^high, by 43% and 62%, respectively, without notable influence on CD11b^+Ly-6G^+ neutrophils. These results suggest that rIL-19 treatment attenuates macrophage recruitment accompanying by increased circulating inflammatory monocytes.

rIL-19 Influences Mediator mRNA Expression in BMDMs

BMDMs were exposed to lipopolysaccharide or interleukin-4, in the presence or absence of rIL-19, to evaluate pro- and anti-inflammatory mediator mRNA
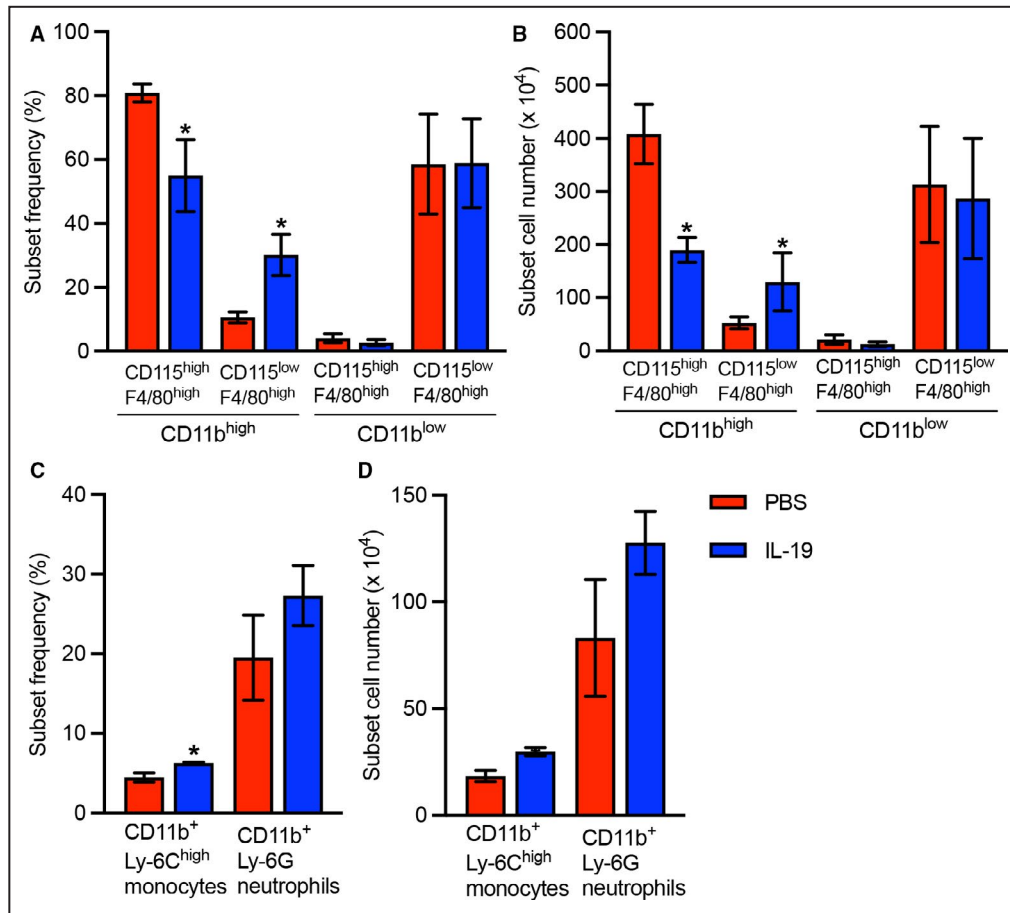
Figure 5. Influence of recombinant interleukin (rIL)-19 treatment on peritoneal macrophage recruitment, circulating inflammatory monocytes and neutrophils.

Male C57BL/6J mice were intraperitoneally injected 1 mL of 3% Brewer thioglycolate medium and daily treated with rIL-19 (10 ng/g body weight) or vehicle (PBS). Four days thereafter, peritoneal cells and tail vein whole blood were collected, counted for leukocytes, stained with monoclonal antibodies against CD11b, CD115, and F4/80 for peritoneal cells or with monoclonal antibodies against CD11b, Ly-6C, and Ly-6G for whole blood, and analyzed on a flow cytometer. **A** and **B**, Mean and standard error of relative (**A**) and absolute (**B**) numbers of individual subsets of peritoneal macrophages defined by CD11b, F4/80, and CD115 expression levels. **C** and **D**, Mean and standard error of relative (**C**) and absolute (**D**) numbers of circulating inflammatory monocytes (CD11b⁺Ly-6Cʰⁱᵍʰ) and neutrophils (CD11b⁺Ly-6G⁺). Student's *t* test, *$P < 0.05$ compared with PBS treatment. n=4 mice per group.

expression in response (Figure 6). Expectedly, inducible nitric oxide synthase, CCL2, MMP2, MMP9, and interleukin-1β mRNA expression was significantly increased in M lipopolysaccharide macrophages. Conversely, TGF-β1 mRNA expression was increased in M interleukin-4. mRNA expression of inducible nitric oxide synthase and CCL2 in M lipopolysaccharide macrophages and interleukin-1β in M interleukin-4 macrophages, respectively, were significantly reduced following exposure to rIL-19. MMP2 and MMP9 expression were significantly attenuated as well, regardless of macrophage activation status (lipopolysaccharide versus interleukin-4). TGF-β1 expression increased in both M lipopolysaccharide macrophages and M interleukin-4 macrophages, but significance was reached only for

M lipopolysaccharide macrophages. Thus, rIL-19 modulates expression of multiple macrophage-derived mediators thought to be relevant to AAA pathogenesis.

Cytokine-Producing or Treg Cells are Minimally Influenced by rIL-19

Given the importance of T-cell–derived cytokines in AAA pathogenesis,[34] the influence of rIL-19 on the functional differentiation of CD4⁺ and CD8⁺ T cells was assessed via flow cytometry-based intracellular cytokine and Foxp3 staining. As shown in Figure 7, more interferon-γ than interleukin-10- or –17A-production was present in both CD4⁺ and CD8⁺ cells, regardless of rIL-19 exposure statues. rIL-19 administration
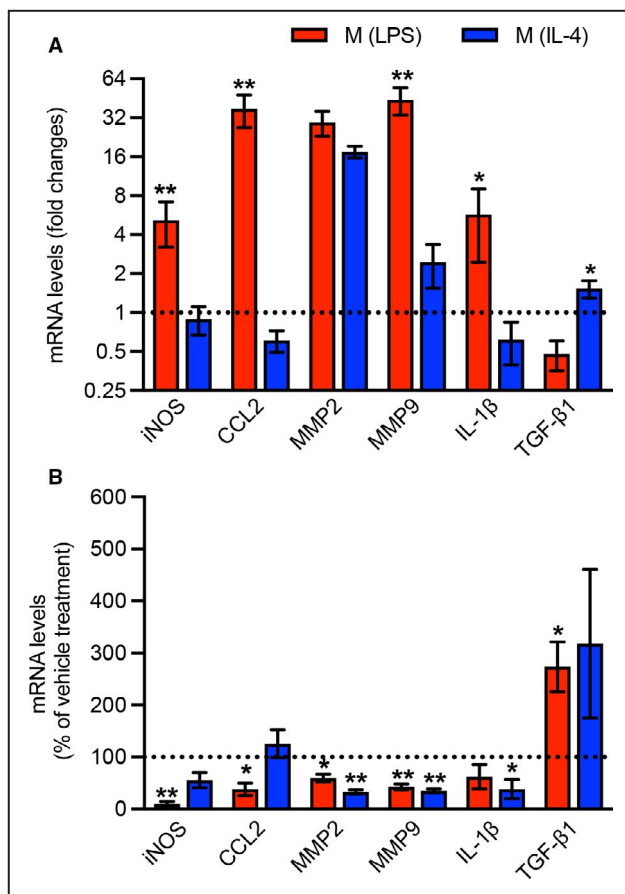
Figure 6. **Recombinant (rIL)-19 alters mRNA expression of macrophage-derived pro- and anti-aneurysmal mediators.** Bone marrow-derived macrophages (BMDMs) from macrophage colony stimulating factor (M-CSF)-differentiated C57BL/6J mouse bone marrow cells were activated with either lipopolysaccharide (LPS) (20 ng/mL) for macrophage (M) (LPS) or interleukin (IL)-4 (20 ng/mL) for M (IL-4), in the presence or absence of IL-19. Massager ribonucleic acids (mRNAs) for pro-, and anti-, inflammatory mediators were quantitated via real-time quantitative reverse transcription-polymerase chain reaction (RT-PCR). **A**, mRNA levels (mean and SE, n=4) in M (LPS) and M (IL-4) macrophages were fold changes relative to BMDMs with vehicle. One sample T-test, *P<0.05 and **P<0.01 compared with BMDMs with vehicle treatment where the mRNA levels are 1. **B**, Message RNA levels (mean and standard error, n=4) in IL-19-treated M (LPS) or M (IL-4) macrophages were presented as the percentage of that in M (LPS) or M (IL-4) with vehicle treatment, where the mRNA levels are 100. One sample T-test, *P<0.05 and **P<0.05 compared with 100 (mRNA levels in vehicle-treated M (LPS) or M (IL-4) macrophages). Dotted lines in (**A**) and (**B**) indicate the mRNA levels in macrophages in the absence of LPS, IL-4 or IL-19. CCL2, C-C motif chemokine ligand 2; iNOS, inducible nitric oxide synthase; MMP, matrix metalloproteinase; and TGF, transforming growth factor.

did increase the population of IL-10-producing CD8+ T cells. Additionally, no difference was noted for splenic or aortic Treg cells between the 2 treatment groups. On the basis of these experiments, neither T-cell–derived cytokines nor Treg cell population appear to modulate rIL-19–mediated AAA suppression.

Interleukin-19 Treatment Impacts Further Progression of Existing AAAs

To further investigate its translational value, rIL-19 was administered to an additional mouse AAA cohort 4 days following PPE infusion, the time point by which aneurysms are formed in this model. In vehicle-treated mice, aneurysms enlarged continuously from days 3 to 14. In contrast, rIL-19 administration reduced, or even regressed, progression of existing AAAs (Figures 8A and 8B). Histologically, rIL-19 was associated with preserved medial elastin and SMCs, reduced mural neovascularization, and attenuated aortic macrophage, T-cell, and B-cell accumulation (Figures 8C and 8D). Taken together, these data suggest that rIL-19, in addition to suppressing aneurysm formation, effectively limits progression of existing AAAs in this modeling system.

IL-19 Treatment Attenuates Angiotensin II–Induced AAAs in Hyperlipidemic Mice

To further assess the potential translational value of these findings, rIL-19 was tested in an alternative experimental AAA model. In angiotensin II/apolipoprotein E knockout mice, rIL-19 administration was associated with reduced suprarenal aortic enlargement and lowered AAA incidence (Figures 9A and 9B). The vast majority of rIL-19–treated mice developed grade II aneurysms as compared with grade IV (≥2) AAAs predominating in vehicle-treated mice (Figure 9C). The average aneurysm severity score was significantly reduced in rIL-19–treated mice (Figure 9D). Additionally, rIL-19 substantially reduced aneurysm rupture; 90% of rIL-19–treated mice survived as compared with 55% in the vehicle-treatment group (Figure 9E). Autopsy confirmed that all deaths were attributable to suprarenal aortic aneurysm rupture. These results confirm that rIL-19–induced AAA suppression is not limited to a single experimental AAA modeling system, and that in angiotensin II–induced aneurysm model, rIL-19 protects against aneurysm rupture and rupture-related mortality in addition to limiting diameter enlargement.

DISCUSSION

Expression of the cytokine IL-19 is increased in clinical and experimental AAAs. Parenteral administration of rIL-19 limited the formation and progression of new and existing experimental AAAs in complementary experimental modeling systems. rIL-19–induced AAA suppression was associated with markedly reduced mural leukocyte accumulation, neoangiogenesis, and substantially downregulated expression of proaneurysmal MMP2, MMP9, and CCL2. These results were neither intuitive nor predictable, as rIL-19 can augment or limit inflammation, depending on the specific circumstances
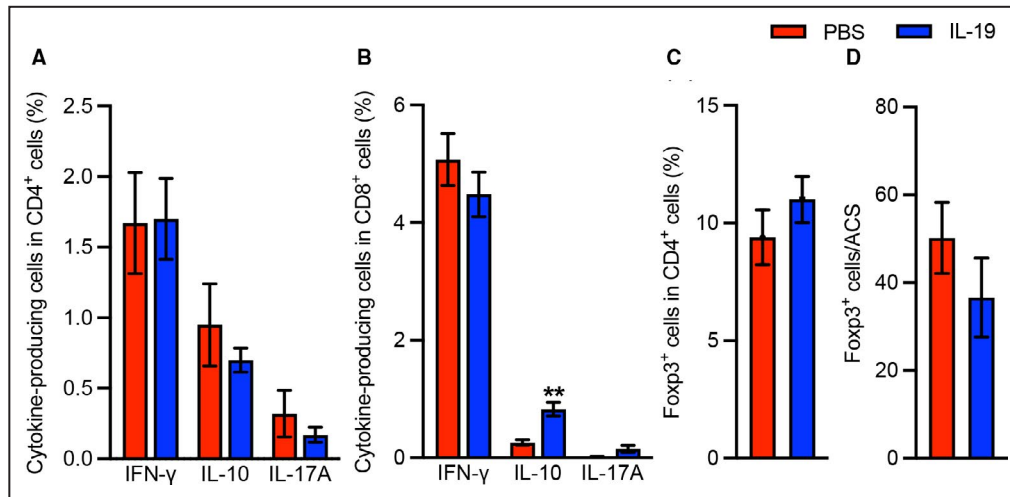
Figure 7. Influence of recombinant interleukin (rIL)-19 treatment on differentiation of cytokine-producing and regulatory T cells.

Lymphocytes were prepared from the spleens of interleukin (IL)-19– (10 ng/g per day) or PBS-treated mice 2 weeks after porcine pancreatic elastase infusion. Cytokine-producing CD4+ (**A**) or CD8+ T cells (**B**) as well as Forkhead box protein P3 (Foxp3)-expressing regulatory CD4+ T cells in spleen (**C**) and aorta (**D**) were detected using intracellular staining and flow cytometric analyses (**A** through **C**) or immunohistochemistry (**D**). Results are tabulated as mean and standard error of the percentages of individual cytokine-producing CD4+ and CD8+ T cells and Foxp3-expressing cells in CD4+ T cells, or Foxp3+ cells/aortic cross-section (ACS). Nonparametric Mann-Whitney test, **P<0.01 between 2 groups. n=5–9 mice/group. IFN indicates interferon.

in which it is expressed.[19–22,31,35–38,23,39–41] In the experimental AAA constructs described herein, rIL-19 administration unequivocally limits disease progression and rupture-related mortality.

The influence of cytokine expression in experimental AAA pathogenesis remains incompletely understood. Aneurysm inhibition has previously been associated with TGF-β1 expression,[14–16] as well as that of interferon-γ and interleukin-12p40 in specific circumstances.[42–44] Interleukin-19 promotes TGF-β expression in tumor and epithelial cells.[45,46] Interleukin-1β, interleukin-6, interferon-γ and tumor necrosis factor-α, all capable of inducing interleukin-19, are all abundantly expressed in aneurysmal aortas,[1] and interleukin-19 also causes autocrine interleukin-19 production by mononuclear and vascular cells.[45,47] In these experiments, interleukin-19 increased TGF-β1 mRNA expression in activated BMDMs, although not to a significant extent in following interleukin-4 activation. Further studies investigating the relationship between interleukin-19, TGF-β, and potential crosstalk between the 2 cytokines during AAA pathogenesis are clearly warranted.

Several candidate mechanisms for interleukin-19–mediated AAA suppression are suggested by these results. rIL-19 administered before and after PPE infusion diminished aortic mural macrophage accumulation by ≈80% and 60%, respectively, in developing AAAs. C-C chemokine receptor 2–expressing

circulating monocytes, recruited in response to CCL2 ligand expression in target tissues, represent the principal source of the aortic mural macrophages in AAAs.[4,48–50] In the present study, rIL-19 administration attenuated both aortic CCL2 protein and macrophage CCL2 mRNA expression, consistent with previous responses in cultured BMDMs, human peripheral blood, and synovial mononuclear cells.[21,51]

Peritoneal macrophage accumulation was suppressed with resultant increase in circulating inflammatory monocytes in response to intraperitoneal thioglycolate, underscoring the potential significance of impaired macrophage recruitment in the observed antianeurysmal effects of rIL-19. Interleukin-19 has also been reported to downregulate intercellular adhesion molecule-1, vascular cell adhesion molecule-1, and E-selectin expression by endothelial cells, thus inhibiting leukocyte adhesion and rolling on endothelial surfaces.[52] Thus, rIL-19–mediated suppression of CCL2 and adhesion molecules critical for leukocyte migration may contribute to reduced aortic macrophage accumulation and thus aneurysm inhibition.

Aortic mural capillary formation, or neovascularization, provides portals for circulating inflammatory monocytes to infiltrate the aortic wall. Pharmacological or genetic manipulation of aortic mural neoangiogenesis, primarily targeting vascular endothelial growth factor-A/hypoxia-inducible factor-1 and related proangiogenic pathways, has provided important insights
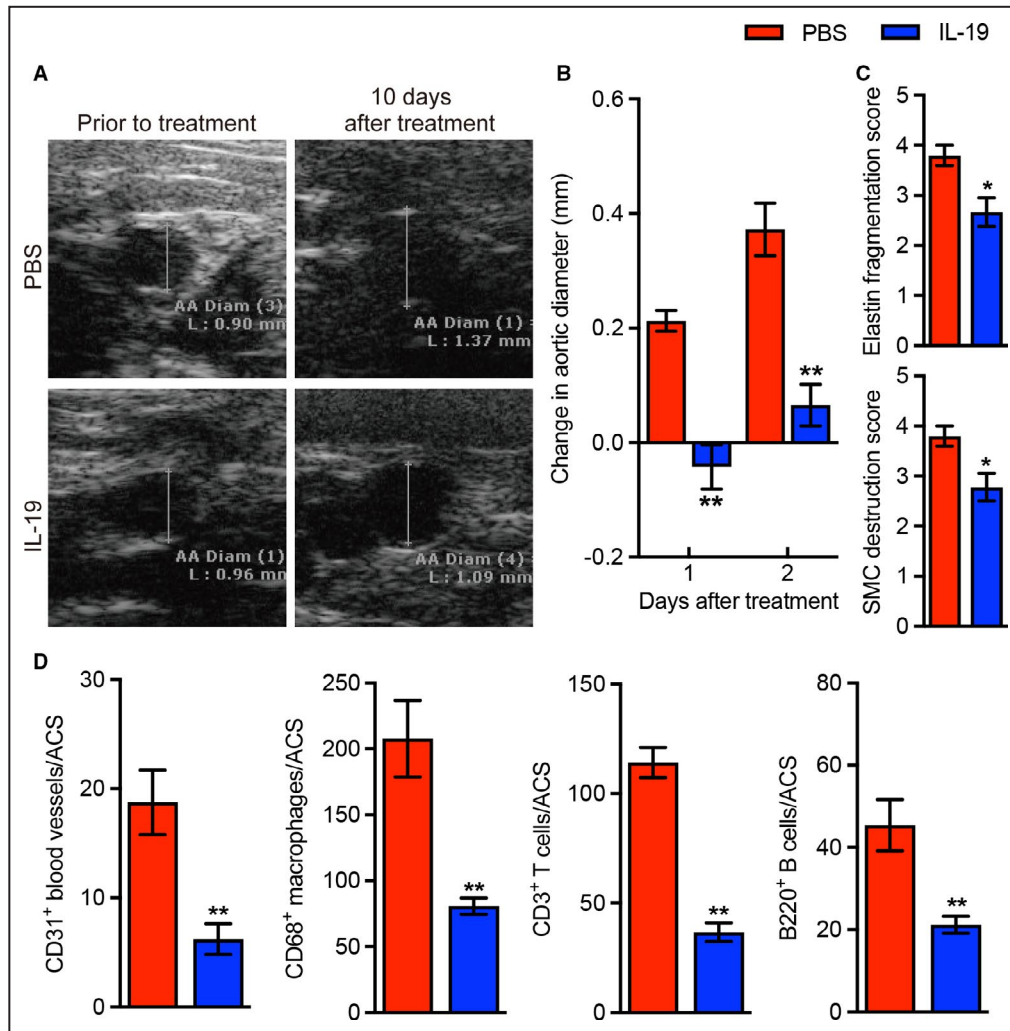
Figure 8.   Recombinant interleukin (rIL)-19 limits further enlargement of existing aneurysms.
Treatment with interleukin (IL)-19 (10 ng/g per day) or PBS initiated 4 days after porcine pancreatic elastase (PPE) infusion and continued for 10 days (n=5-9 mice). Infrarenal aortic diameters were measured 1 day before, and 3 and 10 days after, initiation of treatment. Mice were sacrificed 2 weeks after PPE infusion, and aortic sections were prepared for histopathology. **A**, Representative aortic ultrasound images from IL-19– or PBS-treated, PPE-infused mice before, and 10 days after, initiating treatment. **B**, Mean and Standard error (SE) of delta changes in aortic diameters over aortic diameter 1 day before the treatment. Analysis of variance followed by 2 group comparison test, *$P<0.05$ and **$P<0.01$ compared with PBS treatment at the same time point. **C**, Semiquantitative analysis (mean and SE) of medial elastin fragmentation and smooth-muscle cell (SMC) destruction as evaluated by histology grading system (score I to IV). Nonparametric Mann-Whitney test, *$P<0.05$ compared with PBS treatment. **D**, Quantification of mural macrophages (CD68), T cells (CD3), B cells (B220), and neovessels/angiogenesis (CD31). Data are mean and SE of the numbers of macrophages, T cells, B cells, and neovessels per aortic cross section (ACS). Nonparametric Mann-Whitney test, **$P<0.01$ compared with PBS treatment. n=5–9 mice/group. AA Diam indicates abdominal aortic diameter.

into the central role neoangiogenesis plays in AAA pathogenesis.[27,30,53–58] In this study, mural neovessel density decreased by >60% in treated mice regardless of the timing of rIL-19 administration. Thus, inhibition of mural angiogenesis may represent another suppressive mechanism of rIL-19 on experimental AAA progression.

These antiangiogenic responses, however, are inconsistent with results reported previously in a Matrigel assay and rodent hind limb ischemia model. In the latter

2 settings, the expression of MMPs, CCL2, vascular endothelial growth factor-A, and other proangiogenic factors were augmented in response to rIL-19, accelerating angiogenesis without influencing macrophage cellularity.[36,37,59] In the current experiments, rIL-19 administration remarkably reduced aortic mural macrophage density in conjunction with decreased CCL2, MMP2, and MMP9 expression, all responses cumulating in angiogenesis suppression. Further investigations are
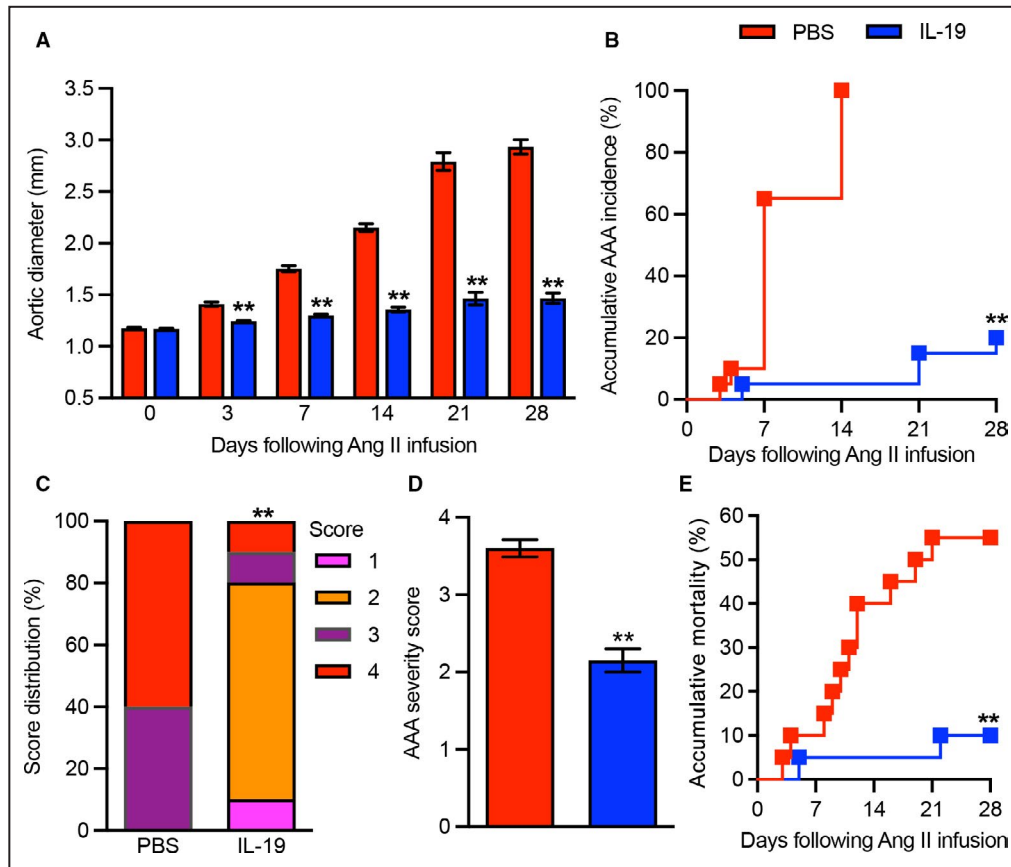
Figure 9. Recombinant interleukin (rIL)-19 limits progression of angiotensin II (Ang II)–induced abdominal aortic aneurysms (AAAs) in hyperlipidemic mice.

AAAs were induced in 10- to 12-week-old male apolipoprotein E (ApoE) knockout (KO) BALB/ mice by subcutaneous infusion of Ang II (1000 ng/min per kg) via an osmotic mini-pump for 4 weeks, and assessed via serial measurements of maximal suprarenal aortic diameter. Interleukin (IL)-19 (10 ng/g body weight) or an equal volume of vehicle (PBS) were administered intraperitoneally to mice 1 day prior to Ang II infusion and 28 days thereafter (n=20 mice/group). **A**, Mean and standard error of suprarenal aortic diameter. Repeated measures 2-way analysis of variance followed by 2 group comparison test at the same time point between 2 treatments. **B**, Cumulative AAA incidence. AAA defined as a ≥50% increase in aortic dimeter over the baseline level, the presence of aortic dissection, or death caused by aneurysm rupture. The log-rank test, **$P<0.01$ compared with vehicle treatment. **C**, Distribution of aneurysm severity score. AAA was graded as score I to V based on the presence of intramural thrombus as well as the shape and number of aneurysms. Chi-square test, **$P<0.01$ compared with PBS treatment. **D**, Mean and standard error of aneurysm severity score. Nonparametric Mann-Whitney test, **$P<0.01$ compared with PBS treatment. **E**, Cumulative mortality due to aneurysm rupture. The log-rank test, **$P<0.01$ compared with vehicle treatment.

needed to understand the idiosyncratic and apparently model-specific response of angiogenesis to IL-19 administration in these disparate experimental conditions.

The contribution of MMP activity to aneurysm pathogenesis has been well documented in AAA disease.[60,61] In the present study, rIL-19 administration reduced MMP2 and MMP9 proteins in AAAs, as well as mRNA expression of both in either classically or alternatively activated BMDMs in vitro. Thus, in addition to limiting MMP-producing macrophage density, reduced macrophage MMP mRNA expression may serve an additional mechanism for interleukin-19–mediated AAA suppression.

T cells, including helper T 1, helper T 2, helper T 17, and Treg cells, influence AAA pathogenesis by producing pro- and anti-inflammatory cytokines.[1] In whole splenic tissue, interferon-γ, interleukin-17, T-bet, and retinoic acid receptor–related orphan receptor c mRNA expression were downregulated, and interleukin-4, interleukin-10, GATA3, and Foxp3 were upregulated in response to rIL-19.[31] In the present study, interleukin-19 altered neither interferon-γ nor interleukin-17 production by splenic $CD4^+$ or $CD8^+$ T cells, or the density of Treg cells in the spleen or aneurysmal aortas. Although rIL-19 administration slightly increased interleukin-10-expressing splenic $CD8^+$ T cells in aneurysmal mice,

the link between increased interleukin-10–producing CD8^{+} T cells and interleukin-19–mediated AAA suppression is uncertain. Thus, the influence of rIL-19 on T-cell differentiation or Treg cells in experimental AAA pathogenesis remains indeterminate.

Although interleukin-19 and interleukin-10 influence intracellular signaling through distinct heterodimer receptors,[19] treatment with rIL-10, or an interleukin-10 transcribing nonimmunogenic viral vector, also mitigated experimental AAAs.[18,62] Deficiency of interleukin-10 promotes angiotensin II–induced AAA progression.[63] As demonstrated for rIL-19 in this study, rIL-10 treatment also reduced CCL2 expression in aneurysmal aorta,[62] suggesting CCL2 as a potential common target for both cytokines. However, differences remain regarding the mechanisms by which both interleukin-19 and interleukin-10 limit experimental AAA progression. rIL-10 promoted M2 macrophage dominance by impeding M1 and boosting M2 polarization.[18,62] In contrast, in these experiments, rIL-19 attenuated proaneurysmal inducible nitric oxide synthase and CCL2 expression in M1 macrophages, reduced interleukin-1β expression in M2 macrophages, downregulated MMP2 and MMP9 expression in both, and increased antianeurysmal TGF-1β expression in M1 but not M2. Additional differential effects of rIL-10 and rIL-19 are apparent by their influence on aortic Treg activity or cellularity,[18,63] with little noted in the current experiments.

AAA disease progresses at an idiosyncratic rate, punctuated by periods of enlargement and quiescence. In the absence of effective drug therapy for early disease, periodic imaging surveillance is required until aneurysms become symptomatic or reach sufficient diameter for surgical repair.[64,65] Identifying a safe, effective, and well-tolerated medical therapy to reduce the rate of AAA disease progression remains one of the most compelling needs in vascular disease management.[66,67] The present results suggest that immune modulation strategies such as interleukin-19 therapy or related interventions may be worthy of clinical evaluation in this application.

Cytokines, including TGF-β1 and interleukin-2, -10, -19, and -33, have proven to be effective immune modulating agents in preclinical AAA models.[62,68–76] Significant challenges remain in translating these findings into safe and effective clinical strategies, however, including concerns regarding duration of efficacy, toxicity, and individual cytokine-specific adverse effects. For example, the translational value of TGF-β1–induced immune suppression is limited by its profibrogenetic effects.[77] Alternatives to extend the half-life of cytokine-based interventional agents while reducing their off-target toxicity are being explored such as engineering cytokine/cytokine antibody fusion,[78] encapsulating cytokines into layer-by-layer assembled nanoparticles[79] and altering cytokine conformational state.[80] Thus, it warrants further investigating the translational feasibility leveraging these innovative strategies for delivering aneurysm cytokine therapy.

Appropriate interpretation of these results depends on recognition of several limitations. First, since the primary intervention was rIL-19 administration, the role of endogenously produced interleukin-19 in AAA pathogenesis was not evaluable in this construct. While the finding of increased interleukin-19 expression in human and experimental AAAs in combination with the observed rIL-19 effects certainly suggests such a role, the experimental design precluded such an assessment. Further studies employing mice deficient for, or who have received blocking agents for, interleukin-19 or its specific receptor may provide more insight into this question. Second, the cell type(s) responsible for increased interleukin-19 expression in both clinical and experimental AAA remain undetermined. Finally, since cytokines are rarely expressed or act as individual mediators, the relationship between interleukin-19 and coexpressed TGF-β1 and interleukin-10 in clinical and experimental AAA pathogenesis also requires more comprehensive assessment to determine the relative contribution of each working in concert to limit aneurysm formation.

In conclusion, rIL-19 administration limits initiation and progression of experimental AAA disease. Further investigation of additional mechanism(s) responsible for this limitation may provide insight into novel methods of limiting clinical AAA disease progression.

ARTICLE INFORMATION

Affiliations

Divison of Vascular Surgery, Department of Surgery, Stanford University School of Medicine, Stanford, CA (H.T., B.X., H.X., Y.L., J.G., S.Z., K.J.G., X.Z., N.F., Y.F., T.I., T.S., R.L.D.); Division of Vascular Surgery, Hamamatsu University School of Medicine, Hamamatsu, Shizuoka, Japan (H.T., K.I., N.U.); Department of Physiology, Nanjing Medical University, Nanjing, Jiangsu, China (Y.G.); Peking University Third Hospital, Medical Research Center, Haidian, Beijing, China (Y.W.); Department of Surgery, Xiangya Hospital, South Central University School of Medicine, Changsha, Hunan, China (W.W., S.L., J.H.); and Department of Vascular Surgery, Zhongshan Hospital, Fudan University, Shanghai, China (L.W., W.F.)..

Sources of Funding

REFERENCES

1. Golledge J. Abdominal aortic aneurysm: update on pathogenesis and medical treatments. *Nat Rev Cardiol*. 2019;16:225–242. DOI: 10.1038/s41569-018-0114-9.

2. Newby D, Forsythe R, McBride O, Robson J, Vesey A, Chalmers R, Burns P, Garden OJ, Semple S, Dweck M, et al. Aortic wall inflammation predicts abdominal aortic aneurysm expansion, rupture, and need for surgical repair. *Circulation*. 2017;136:787–797. DOI: 10.1161/CIRCULATIONAHA.117.028433.

3. Paige E, Clément M, Lareyre F, Sweeting M, Raffort J, Grenier C, Finigan A, Harrison J, Peters JE, Sun BB, et al. Interleukin-6 receptor signaling and abdominal aortic aneurysm growth rates. *Circ Genom Precis Med*. 2019;12:e002413. DOI: 10.1161/CIRCGEN.118.002413.

4. Ishibashi M, Egashira K, Zhao Q, Hiasa K-I, Ohtani K, Ihara Y, Charo IF, Kura S, Tsuzuki T, Takeshita A, et al. Bone marrow-derived monocyte chemoattractant protein-1 receptor CCR2 is critical in angiotensin II-induced acceleration of atherosclerosis and aneurysm formation in hypercholesterolemic mice. *Arterioscler Thromb Vasc Biol*. 2004;24:e174–178. DOI: 10.1161/01.ATV.0000143384.69170.2d.

5. Batra R, Suh MK, Carson JS, Dale MA, Meisinger TM, Fitzgerald M, Opperman PJ, Luo J, Pipinos II, Xiong W, et al. Il-1beta (interleukin-1beta) and TNF-alpha (tumor necrosis factor-alpha) impact abdominal aortic aneurysm formation by differential effects on macrophage polarization. *Arterioscler Thromb Vasc Biol*. 2018;38:457–463.

6. Wei Z, Wang YU, Zhang K, Liao Y, Ye P, Wu J, Wang Y, Li F, Yao Y, Zhou Y, et al. Inhibiting the Th17/IL-17A-related inflammatory responses with digoxin confers protection against experimental abdominal aortic aneurysm. *Arterioscler Thromb Vasc Biol*. 2014;34:2429–2438. DOI: 10.1161/ATVBAHA.114.304435.

7. Sharma AK, Lu G, Jester A, Johnston WF, Zhao Y, Hajzus VA, Saadatzadeh MR, Su G, Bhamidipati CM, Mehta GS, et al. Experimental abdominal aortic aneurysm formation is mediated by IL-17 and attenuated by mesenchymal stem cell treatment. *Circulation*. 2012;126:S38–S45. DOI: 10.1161/CIRCULATIONAHA.111.083451.

8. Xiong W, MacTaggart J, Knispel R, Worth J, Persidsky Y, Baxter BT. Blocking TNF-alpha attenuates aneurysm formation in a murine model. *J Immunol*. 2009;183:2741–2746.

9. Zhou HF, Yan H, Cannon JL, Springer LE, Green JM, Pham CT. CD43-mediated IFN-gamma production by CD8+ T cells promotes abdominal aortic aneurysm in mice. *J Immunol*; 2013;190:5078–5085.

10. Iida Y, Xu B, Xuan H, Glover KJ, Tanaka H, Hu X, Fujimura N, Wang W, Schultz JR, Turner CR, et al. Peptide inhibitor of CXCL4-CCL5 heterodimer formation, MKEY, inhibits experimental aortic aneurysm initiation and progression. *Arterioscler Thromb Vasc Biol*. 2013;33:718–726. DOI: 10.1161/ATVBAHA.112.300329.

11. Moehle CW, Bhamidipati CM, Alexander MR, Mehta GS, Irvine JN, Salmon M, Upchurch GR Jr, Kron IL, Owens GK, Ailawadi G. Bone marrow-derived MCP1 required for experimental aortic aneurysm formation and smooth muscle phenotypic modulation. *J thorac Cardiovasc Surg*. 2011;142:1567–1574. DOI: 10.1016/j.jtcvs.2011.07.053.

12. Harrison SC, Smith AJP, Jones GT, Swerdlow DI, Rampuri R, Bown MJ, Folkersen L, Baas AF, de Borst GJ, Blankensteijn JD, et al. Interleukin-6 receptor pathways in abdominal aortic aneurysm. *Eur Heart J*. 2013;34:3707–3716. DOI: 10.1093/eurheartj/ehs354.

13. Kokje VBC, Gabel G, Dalman RL, Koole D, Northoff BH, Holdt LM, Hamming JF, Lindeman JHN. CXCL8 hyper-signaling in the aortic abdominal aneurysm. *Cytokine*. 2018;108:96–104. DOI: 10.1016/j.cyto.2018.03.031.

14. Angelov SN, Hu JH, Wei H, Airhart N, Shi M, Dichek DA. TGF-beta (transforming growth factor-beta) signaling protects the thoracic and abdominal aorta from angiotensin II-induced pathology by distinct mechanisms. *Arterioscler Thromb Vasc Biol*. 2017;37:2102–2113.

15. Wang Y, Ait-Oufella H, Herbin O, Bonnin P, Ramkhelawon B, Taleb S, Huang J, Offenstadt G, Combadiere C, Renia L, et al. TGF-beta activity protects against inflammatory aortic aneurysm

16. progression and complications in angiotensin II-infused mice. *J Clin Investig*. 2010;120:422–432.

16. Dai J, Losy F, Guinault AM, Pages C, Anegon I, Desgranges P, Becquemin JP, Allaire E. Overexpression of transforming growth factor-beta1 stabilizes already-formed aortic aneurysms: a first approach to induction of functional healing by endovascular gene therapy. *Circulation*. 2005;112:1008–1015.

17. Li J, Xia NI, Wen S, Li D, Lu Y, Gu M, Tang T, Jiao J, Lv B, Nie S, et al. IL (interleukin)-33 suppresses abdominal aortic aneurysm by enhancing regulatory T-cell expansion and activity. *Arterioscler Thromb Vasc Biol*. 2019;39:446–458. DOI: 10.1161/ATVBAHA.118.312023.

18. Adam M, Kooreman NG, Jagger A, Wagenhäuser MU, Mehrkens D, Wang Y, Kayama Y, Toyama K, Raaz U, Schellinger IN, et al. Systemic upregulation of IL-10 (interleukin-10) using a nonimmunogenic vector reduces growth and rate of dissecting abdominal aortic aneurysm. *Arterioscler Thromb Vasc Biol*. 2018;38:1796–1805. DOI: 10.1161/ATVBAHA.117.310672.

19. Rutz S, Wang X, Ouyang W. The IL-20 subfamily of cytokines–from host defence to tissue homeostasis. *Nat Rev Immunol*. 2014;14:783–795.

20. Ellison S, Gabunia K, Richards JM, Kelemen SE, England RN, Rudic D, Azuma YT, Munroy MA, Eguchi S, Autieri MV. IL-19 reduces ligation-mediated neointimal hyperplasia by reducing vascular smooth muscle cell activation. *Am J Pathol*. 2014;184:2134–2143. DOI: 10.1016/j.ajpath.2014.04.001.

21. Gabunia K, Ellison S, Kelemen S, Kako F, Cornwell WD, Rogers TJ, Datta PK, Ouimet M, Moore KJ, Autieri MV. IL-19 halts progression of atherosclerotic plaque, polarizes, and increases cholesterol uptake and efflux in macrophages. *Am J Pathol*. 2016;186:1361–1374. DOI: 10.1016/j.ajpath.2015.12.023.

22. Xie W, Fang L, Gan S, Xuan H. Interleukin-19 alleviates brain injury by anti-inflammatory effects in a mice model of focal cerebral ischemia. *Brain Res*. 2016;1650:172–177. DOI: 10.1016/j.brainres.2016.09.006.

23. An W, Yu Y, Zhang Y, Zhang Z, Yu Y, Zhao X. Exogenous IL-19 attenuates acute ischaemic injury and improves survival in male mice with myocardial infarction. *Br J Pharmacol*. 2019;176:699–710. DOI: 10.1111/bph.14549.

24. Autieri MV. IL-19 and other IL-20 family member cytokines in vascular inflammatory diseases. *Front Immunol*. 2018;9:700. DOI: 10.3389/fimmu.2018.00700.

25. Groeneveld ME, Meekel JP, Rubinstein SM, Merkestein LR, Tangelder GJ, Wisselink W, Truijers M, Yeung KK. Systematic review of circulating, biomechanical, and genetic markers for the prediction of abdominal aortic aneurysm growth and rupture. *J Am Heart Assoc*. 2018;7:e007791. DOI: 10.1161/JAHA.117.007791.

26. Iida Y, Xu B, Schultz GM, Chow V, White JJ, Sulaimon S, Hezi-Yamit A, Peterson SR, Dalman RL. Efficacy and mechanism of angiotensin II receptor blocker treatment in experimental abdominal aortic aneurysms. *PLoS One*. 2012;7:e49642. DOI: 10.1371/journal.pone.0049642.

27. Xu B, Iida Y, Glover KJ, Ge Y, Wang Y, Xuan H, Hu X, Tanaka H, Wang W, Fujimura N, et al. Inhibition of VEGF (vascular endothelial growth factor)-A or its receptor activity suppresses experimental aneurysm progression in the aortic elastase infusion model. *Arterioscler Thromb Vasc Biol*. 2019;39:1652–1666. DOI: 10.1161/ATVBAHA.119.312497.

28. Xuan H, Xu B, Wang W, Tanaka H, Fujimura N, Miyata M, Michie SA, Dalman RL. Inhibition or deletion of angiotensin II type 1 receptor suppresses elastase-induced experimental abdominal aortic aneurysms. *J Vasc Surg*. 2018;67:573–584.e572.

29. Daugherty A, Manning MW, Cassis LA. Angiotensin II promotes atherosclerotic lesions and aneurysms in apolipoprotein E-deficient mice. *J Clin Investig*. 2000;105:1605–1612. DOI: 10.1172/JCI7818.

30. Wang W, Xu B, Xuan H, Ge Y, Wang Y, Wang L, Huang J, Fu W, Michie SA, Dalman RL. Hypoxia-inducible factor 1 in clinical and experimental aortic aneurysm disease. *J Vasc Surg*. 2018;68:1538–1550.e1532. DOI: 10.1016/j.jvs.2017.09.030.

31. Ellison S, Gabunia K, Kelemen SE, England RN, Scalia R, Richards JM, Orr AW, Traylor JG, Rogers T, Cornwell W, et al. Attenuation of experimental atherosclerosis by interleukin-19. *Arterioscler Thromb Vasc Biol*. 2013;33:2316–2324. DOI: 10.1161/ATVBAHA.113.301521.

32. Murray P, Allen J, Biswas S, Fisher E, Gilroy D, Goerdt S, Gordon S, Hamilton J, Ivashkiv L, Lawrence T, et al. Macrophage activation and polarization: nomenclature and experimental guidelines. *Immunity*. 2014;41:14–20. DOI: 10.1016/j.immuni.2014.06.008.

33. Fujimura N, Xu B, Dalman J, Deng H, Aoyama K, Dalman RL. Ccr2 inhibition sequesters multiple subsets of leukocytes in the bone marrow. *Sci Rep*. 2015;5:11664. DOI: 10.1038/srep11664.

34. Davis FM, Daugherty A, Lu HS. Updates of recent aortic aneurysm research. *Arterioscler Thromb Vasc Biol*. 2019;39:e83–e90. DOI: 10.1161/ATVBAHA.119.312000.

35. Ray M, Gabunia K, Vrakas CN, Herman AB, Kako F, Kelemen SE, Grisanti LA, Autieri MV. Genetic deletion of IL-19 (interleukin-19) exacerbates atherogenesis in IL19(-/-)×Ldlr(-/-) double knockout mice by dysregulation of mRNA stability protein HUR (human antigen R). *Arterioscler Thromb Vasc Biol*. 2018;38:1297–1308.

36. Richards J, Gabunia K, Kelemen SE, Kako F, Choi ET, Autieri MV. Interleukin-19 increases angiogenesis in ischemic hind limbs by direct effects on both endothelial cells and macrophage polarization. *J Mol Cell Cardiol*. 2015;79:21–31. DOI: 10.1016/j.yjmcc.2014.11.002.

37. Jain S, Gabunia K, Kelemen SE, Panetti TS, Autieri MV. The anti-inflammatory cytokine interleukin 19 is expressed by and angiogenic for human endothelial cells. *Arterioscler Thromb Vasc Biol*. 2011;31:167–175. DOI: 10.1161/ATVBAHA.110.214916.

38. Tian Y, Sommerville LJ, Cuneo A, Kelemen SE, Autieri MV. Expression and suppressive effects of interleukin-19 on vascular smooth muscle cell pathophysiology and development of intimal hyperplasia. *Am J Pathol*. 2008;173:901–909. DOI: 10.2353/ajpath.2008.080163.

39. Bruns DR, Ghincea AR, Ghincea CV, Azuma YT, Watson PA, Autieri MV, Walker LA. Interleukin-19 is cardioprotective in dominant negative cyclic adenosine monophosphate response-element binding protein-mediated heart failure in a sex-specific manner. *World J Cardiol*. 2017;9:673–684. DOI: 10.4330/wjc.v9.i8.673.

40. Yeh CH, Cheng BC, Hsu CC, Chen HW, Wang JJ, Chang MS, Hsing CH. Induced interleukin-19 contributes to cell-mediated immunosuppression in patients undergoing coronary artery bypass grafting with cardiopulmonary bypass. *Ann Thorac Surg*. 2011;92:1252–1259. DOI: 10.1016/j.athoracsur.2011.04.061.

41. Hsing CH, Hsieh MY, Chen WY, Cheung So E, Cheng BC, Chang MS. Induction of interleukin-19 and interleukin-22 after cardiac surgery with cardiopulmonary bypass. *Ann Thorac Surg*. 2006;81:2196–2201. DOI: 10.1016/j.athoracsur.2006.01.092.

42. King VL, Lin AY, Kristo F, Anderson TJ, Ahluwalia N, Hardy GJ, Owens AP III, Howatt DA, Shen D, Tager AM, et al. Interferon-gamma and the interferon-inducible chemokine CXCL10 protect against aneurysm formation and rupture. *Circulation*. 2009;119:426–435.

43. Shimizu K, Shichiri M, Libby P, Lee RT, Mitchell RN. Th2-predominant inflammation and blockade of IFN-gamma signaling induce aneurysms in allografted aortas. *J Clin Investig*. 2004;114:300–308.

44. Sharma N, Dev R, Belenchia AM, Aroor AR, Whaley-Connell A, Pulakat L, Hans CP. Deficiency of IL12p40 (interleukin 12 p40) promotes ang II (angiotensin II)-induced abdominal aortic aneurysm. *Arterioscler Thromb Vasc Biol*. 2019;39:212–223. DOI: 10.1161/ATVBAHA.118.311969.

45. Hsu YH, Li HH, Sung JM, Chen WT, Hou YC, Chang MS. Interleukin-19 mediates tissue damage in murine ischemic acute kidney injury. *PLoS One*. 2013;8:e56028. DOI: 10.1371/journal.pone.0056028.

46. Hsing CH, Kwok FA, Cheng HC, Li CF, Chang MS. Inhibiting interleukin-19 activity ameliorates esophageal squamous cell carcinoma progression. *PLoS One*. 2013;8:e75254. DOI: 10.1371/journal.pone.0075254.

47. Jordan WJ, Eskdale J, Boniotto M, Lennon GP, Peat J, Campbell JD, Gallagher G. Human IL-19 regulates immunity through auto-induction of IL-19 and production of IL-10. *Eur J Immunol*. 2005;35:1576–1582. DOI: 10.1002/eji.200425317.

48. de Waard V, Bot I, de Jager SC, Talib S, Egashira K, de Vries MR, Quax PH, Biessen EA, van Berkel TJ. Systemic MCP1/CCR2 blockade and leukocyte specific MCP1/CCR2 inhibition affect aortic aneurysm formation differently. *Atherosclerosis*. 2010;211:84–89. DOI: 10.1016/j.atherosclerosis.2010.01.042.

49. Daugherty A, Rateri DL, Charo IF, Owens AP, Howatt DA, Cassis LA. Angiotensin II infusion promotes ascending aortic aneurysms: attenuation by CCR2 deficiency in ApoE-/- mice. *Clin Sci*. 2010;118:681–689. DOI: 10.1042/CS20090372.

50. MacTaggart JN, Xiong W, Knispel R, Baxter BT. Deletion of CCR2 but not CCR5 or CXCR3 inhibits aortic aneurysm formation. *Surgery*. 2007;142:284–288. DOI: 10.1016/j.surg.2007.04.017.

51. Kragstrup TW, Andersen T, Holm C, Schiottz-Christensen B, Jurik AG, Hvid M, Deleuran B. Toll-like receptor 2 and 4 induced interleukin-19 dampens immune reactions and associates inversely with spondyloarthritis disease activity. *Clin Exp Immunol*. 2015;180:233–242. DOI: 10.1111/cei.12577.

52. England RN, Preston KJ, Scalia R, Autieri MV. Interleukin-19 decreases leukocyte-endothelial cell interactions by reduction in endothelial cell adhesion molecule mRNA stability. *Am J Physiol Cell Physiol*. 2013;305:C255–C265. DOI: 10.1152/ajpcell.00069.2013.

53. Rouer M, Xu BH, Xuan HJ, Tanaka H, Fujimura N, Glover KJ, Furusho Y, Gerritsen M, Dalman RL. Rapamycin limits the growth of established experimental abdominal aortic aneurysms. *Eur J Vasc Endovasc Surg*. 2014;47:493–500. DOI: 10.1016/j.ejvs.2014.02.006.

54. Yang L, Shen L, Li G, Yuan H, Jin X, Wu X. Silencing of hypoxia inducible factor-1alpha gene attenuated angiotensin-induced abdominal aortic aneurysm in apolipoprotein E-deficient mice. *Atherosclerosis*. 2016;252:40–49.

55. Tsai SH, Huang PH, Hsu YJ, Peng YJ, Lee CH, Wang JC, Chen JW, Lin SJ. Inhibition of hypoxia inducible factor-1alpha attenuates abdominal aortic aneurysm progression through the down-regulation of matrix metalloproteinases. *Sci Rep*. 2016;6:28612.

56. Kaneko H, Anzai T, Takahashi T, Kohno T, Shimoda M, Sasaki A, Shimizu H, Nagai T, Maekawa Y, Yoshimura K, et al. Role of vascular endothelial growth factor-a in development of abdominal aortic aneurysm. *Cardiovasc Res*. 2011;91:358–367. DOI: 10.1093/cvr/cvr080.

57. Tedesco MM, Terashima M, Blankenberg FG, Levashova Z, Spin JM, Backer MV, Backer JM, Sho M, Sho E, McConnell MV, et al. Analysis of in situ and ex vivo vascular endothelial growth factor receptor expression during experimental aortic aneurysm progression. *Arterioscler Thromb Vasc Biol*. 2009;29:1452–1457. DOI: 10.1161/ATVBAHA.109.187757.

58. Sho E, Sho M, Nanjo H, Kawamura K, Masuda H, Dalman RL. Hemodynamic regulation of CD34+ cell localization and differentiation in experimental aneurysms. *Arterioscler Thromb Vasc Biol*. 2004;24:1916–1921.

59. Kako F, Gabunia K, Ray M, Kelemen SE, England RN, Kako B, Scalia RG, Autieri MV. Interleukin-19 induces angiogenesis in the absence of hypoxia by direct and indirect immune mechanisms. *Am J Physiol Cell Physiol*. 2016;310:C931–C941. DOI: 10.1152/ajpcell.00006.2016.

60. Longo GM, Xiong W, Greiner TC, Zhao Y, Fiotti N, Baxter BT. Matrix metalloproteinases 2 and 9 work in concert to produce aortic aneurysms. *J Clin Investig*. 2002;110:625–632. DOI: 10.1172/JCI0215334.

61. Pyo R, Lee JK, Shipley JM, Curci JA, Mao D, Ziporin SJ, Ennis TL, Shapiro SD, Senior RM, Thompson RW. Targeted gene disruption of matrix metalloproteinase-9 (gelatinase B) suppresses development of experimental abdominal aortic aneurysms. *J Clin Investig*. 2000;105:1641–1649. DOI: 10.1172/JCI8931.

62. Zhu H, Qu X, Zhang C, Yu Y. Interleukin-10 promotes proliferation of vascular smooth muscle cells by inhibiting inflammation in rabbit abdominal aortic aneurysm. *Int J Clin Exp Pathol*. 2019;12:1260–1271.

63. Ait-Oufella H, Wang YU, Herbin O, Bourcier S, Potteaux S, Joffre J, Loyer X, Ponnuswamy P, Esposito B, Dalloz M, et al. Natural regulatory T cells limit angiotensin ii-induced aneurysm formation and rupture in mice. *Arterioscler Thromb Vasc Biol*. 2013;33:2374–2379. DOI: 10.1161/ATVBAHA.113.301280.

64. Chaikof EL, Dalman RL, Eskandari MK, Jackson BM, Lee WA, Mansour MA, Mastracci TM, Mell M, Murad MH, Nguyen LL, et al. The society for vascular surgery practice guidelines on the care of patients with an abdominal aortic aneurysm. *J Vasc Surg*. 2018;67:2–77.e72. DOI: 10.1016/j.jvs.2017.10.044.

65. Bown MJ, Sweeting MJ, Brown LC, Powell JT, Thompson SG. Surveillance intervals for small abdominal aortic aneurysms: a meta-analysis. *JAMA*. 2013;309:806–813.

66. Golledge J, Norman PE, Murphy MP, Dalman RL. Challenges and opportunities in limiting abdominal aortic aneurysm growth. *J Vasc Surg*. 2017;65:225–233. DOI: 10.1016/j.jvs.2016.08.003.

67. Kraiss LW, Conte MS, Geary RL, Kibbe M, Ozaki CK. Setting high-impact clinical research priorities for the Society for Vascular Surgery. *J Vasc Surg*. 2013;57:493–500. DOI: 10.1016/j.jvs.2012.09.069.

68. Yang P, Schmit BM, Fu C, DeSart K, Oh SP, Berceli SA, Jiang Z. Smooth muscle cell-specific Tgfbr1 deficiency promotes aortic aneurysm formation by stimulating multiple signaling events. *Sci Rep*. 2016;6:35444. DOI: 10.1038/srep35444.

69. Chen X, Rateri DL, Howatt DA, Balakrishnan A, Moorleghen JJ, Cassis LA, Daugherty A. TGF-β neutralization enhances AngII-induced aortic rupture and aneurysm in both thoracic and abdominal regions. *PLoS One*. 2016;11:e0153811. DOI: 10.1371/journal.pone.0153811.

70. Raffort J, Lareyre F, Clément M, Moratal C, Jean-Baptiste E, Hassen-Khodja R, Burel-Vandenbos F, Bruneval P, Chinetti G, Mallat Z. Transforming growth factor β neutralization finely tunes macrophage

phenotype in elastase-induced abdominal aortic aneurysm and is associated with an increase of arginase 1 expression in the aorta. *J Vasc Surg*. 2019;70:588–598.e582. DOI: 10.1016/j.jvs.2018.09.045.

71. Wang Y, Ait-Oufella H, Herbin O, Bonnin P, Ramkhelawon B, Taleb S, Huang J, Offenstadt G, Combadière C, Rénia L, et al. TGF-beta activity protects against inflammatory aortic aneurysm progression and complications in angiotensin II-infused mice. *J Clin Investig*. 2010;120:422–432.

72. Yodoi K, Yamashita T, Sasaki N, Kasahara K, Emoto T, Matsumoto T, Kita T, Sasaki Y, Mizoguchi T, Sparwasser T, et al. Foxp3+ regulatory T cells play a protective role in angiotensin II-induced aortic aneurysm formation in mice. *Hypertension*. 2015;65:889-895.

73. Zhou G, Liao M, Wang F, Qi X, Yang P, Berceli SA, Sharma AK, Upchurch GR Jr, Jiang Z. Cyclophilin a contributes to aortopathy induced by postnatal loss of smooth muscle TGFBR1. *FASEB J*. 2019;33:11396–11410. DOI: 10.1096/fj.201900601RR.

74. Gao F, Chambon P, Offermanns S, Tellides G, Kong W, Zhang X, Li W. Disruption of TGF-β signaling in smooth muscle cell prevents elastase-induced abdominal aortic aneurysm. *Biochem Biophys Res Comm*. 2014;454:137–143. DOI: 10.1016/j.bbrc.2014.10.053.

75. Frutkin AD, Otsuka G, Stempien-Otero A, Sesti C, Du L, Jaffe M, Dichek HL, Pennington CJ, Edwards DR, Nieves-Cintrón M, et al. TGF-[beta]1 limits plaque growth, stabilizes plaque structure, and prevents aortic dilation in apolipoprotein E-null mice. *Arterioscler Thromb Vasc Biol*. 2009;29:1251–1257.

76. Angelov SN, Hu JH, Wei H, Airhart N, Shi M, Dichek DA. Tgf-β (transforming growth factor-β) signaling protects the thoracic and abdominal aorta from angiotensin II-induced pathology by distinct mechanisms. *Arterioscler Thromb Vasc Biol*. 2017;37:2102–2113. DOI: 10.1161/ATVBAHA.117.309401.

77. Budi EH, Schaub JR, Decaris M, Turner S, Derynck R. TGF-β as a driver of fibrosis: physiological roles and therapeutic opportunities. *J Pathol*. 2021.

78. Spangler JB, Trotta E, Tomala J, Peck A, Young TA, Savvides CS, Silveria S, Votavova P, Salafsky J, Pande VS, et al. Engineering a single-agent cytokine/antibody fusion that selectively expands regulatory T cells for autoimmune disease therapy. *J Immunol*. 2018;201:2094–2106.

79. Barberio AE, Smith SG, Correa S, Nguyen C, Nhan B, Melo M, Tokatlian T, Suh H, Irvine DJ, Hammond PT. Cancer cell coating nanoparticles for optimal tumor-specific cytokine delivery. *ACS Nano*. 2020;14:11238–11253. DOI: 10.1021/acsnano.0c03109.

80. De Paula VS, Jude KM, Nerli S, Glassman CR, Garcia KC, Sgourakis NG. Interleukin-2 druggability is modulated by global conformational transitions controlled by a helical capping switch. *Proc Natl Acad Sci USA*. 2020;117:7183–7192. DOI: 10.1073/pnas.2000419117.

SUPPLEMENTAL MATERIAL

Table S1. Major Resources Tables.

Animals (in vivo studies)

Species	Vendor or Source	Background Strain	Sex
Mouse	The Jackson Laboratory	Wilde type C57BL/6J	Male
Mouse	Japan SLC	ApoE-deficient mice on BALB/c genetic background	Male

Antibodies

Target antigen	Vendor or Source	Host (Clone number)	Catalog #	Working concentration	Conjugate
Mouse CD3	Biolegend Inc	Hamster (145-2C11)	100302	2.5 µg/ml	Not conjugated
Mouse B220	Biolegend Inc	Rat (RA3-6B2)	103202	2.5 µg/ml	Not conjugated
Mouse CD68	Biolegend Inc	Rat (FA-11)	137002	2.5 µg/ml	Not conjugated
Mouse CD31	Biolegend Inc	Rat (390)	102402	2.5 µg/ml	Not conjugated
Mouse CD4	Biolegend Inc	Rat (GK1.5)	100422	0.5 µg/ml	PE/Cy7
Mouse CD8	Biolegend Inc	Rat (53-6.7)	100722	0.5 µg/ml	PE/Cy7
Mouse IFN-γ	Biolegend Inc	XMG1.2	505806	5.0 µg/ml	FITC
Mouse IL-10	Biolegend Inc	JES5-16E3	505008	5.0 µg/ml	PE
Mouse IL-17	Biolegend Inc	TC11-18H10.1	506912	5.0 µg/ml	Alexa 647
Mouse CD11b	Biolegend Inc	M1/70	101216	0.05 µg/ml	PE/Cy7
Mouse CD115	Biolegend Inc	AFS98	135510	0.05 µg/ml	APC
Mouse F4/80	Biolegend Inc	BM8	157304	0.1 µg/ml	PE
Mouse Ly-6C	Biolegend Inc	KK1.4	128022	0.125 µg/ml	Alexa 448
Mouse Ly-6G	Biolegend Inc	1A8	127608	0.05 µg/ml	PE
Mouse Foxp3	eBioscience	Rat (FJK-16s)	14-5773-82	5.0 µg/ml	Not conjugated
Mouse Foxp3	Biolegend	Rat (MF-14)	320011	5.0 µg/ml	Alexa 488
Mouse SMC α actin	Thermo Fisher Scientific	Rabbit (IgG)	RB 9010-P	1.0 µg/ml	Not conjugated
Mouse MMP2	Chemicon	Rabbit (IgG)	AB19167	10.0 µg/ml	Not conjugated
Mouse MMP9	Chemicon	Rabbit (IgG)	AB19016	10.0 µg/ml	Not conjugated

Mouse CCL2	Santa Cruz Biotechnology, Inc	Goat (IgG)	SC-1784	2.0 µg/ml	Not conjugated
Mouse and human IL-19	abcam	Rabbit (IgG)	ab198925	57.5 µg/ml	Not conjugated
Rat IgG	Jackson ImmunoResearch	Goat (IgG)	112-065-006	3.5 µg/ml	Biotinylated
Hamster IgG	Jackson ImmunoResearch	Goat (IgG)	107-066-142	7.5 µg/ml	Biotinylated
Rabbit IgG	Jackson ImmunoResearch	Goat (IgG)	111-065-003	3.5 µg/ml	Biotinylated
Goat IgG	Jackson ImmunoResearch	Donkey (IgG)	705-065-003	2.5 µg/ml	Biotinylated

Additional reagents for immunohistochemistry, tissue culture and in vivo treatment

Reagent	Vendor or Source	Host/species	Catalog #	Working concentration	Conjugate
Peroxidase	Jackson ImmunoResearch	N/A	016-030-084	5.0 µg/ml	Streptavidin
Normal mouse serum	Jackson ImmunoResearch	Mouse	015-000-012	4%	Not conjugated
Normal goat serum	Invitrogen	Goat	1000C	10%	Not conjugated
Normal rabbit IgG	R&D Systems	Rabbit	AB-105-C	1.0 µg/ml	Not conjugated
Normal goat IgG	R&D Systems	Goat	AB-108-C	5.0 µg/ml	Not conjugated
AEC peroxidase substrate Kit	Vector Laboratories, Inc	N/A	SK-4200	N/A	N/A
DAB peroxidase substrate kit	Vector Laboratories, Inc	N/A	SK-4100	N/A	N/A
M-CSF	Biolegend Inc	N/A	576406	20 ng/ml	N/A
IL-4	Biolegend Inc	N/A	574306	20 ng/ml	N/A
Mouse IL-19	eBioscience	N/A	14-8191	10 µg/kg/day	N/A
LPS	Sigma-Aldrich Corp	N/A	L6143-1MG	20 ng/ml	N/A
Elastase	Sigma-Aldrich Corp	Porcine pancreas	E-1250-100MG	1.5 units/ml	N/A
Human angiotensin II	Sigma-Aldrich Corp	Synthetic	A9525-50MG	1000 ng/min/kg	N/A
Alzet mini-osmotic minipump	Durect Corp	N/A	Model 2004	N/A	N/A

Table S2. Characteristics for 19 AAA patients.

Variable	Result
Male sex (n, %)	13 (68.4%)
Age (range, mean ± SE, years)	47-81 (65.5 ± 1.8)
Aortic diameter (mm, range, mean ± SE)	35-90 (61.8 ± 3.3)
Luminal thrombus (n, %)	13 (68.4%)
Smoker (n, %)	6 (31.6%)
Hypertension (n, %)	9 (47.4%)
Hyperlipidemia (n, %)	3 (15.8%)
Diabetes (n, %)	4 (21.1%)
COPD (n, %)	0 (0.0%)
Antihypertension medication	7 (36.8%)
Lipid-lowering medication	1 (5.3%)
Antidiabetic medication	2 (10.5%)

SD: Standard error. COPD: chronic obstructive pulmonary disease

Table S3. Primer sequences used for real-time quantitative RT-PCR assay.

Gene	Sequence
iNOS	CGA AAC GCT TCA CTT CCA A
	TGA GCC TAT ATT GCT GTG GCT
CCL2	TAA AAA CCT GGA TCG AAC CAA A
	GCA TTA GCT TCA CAT TTA CGG GT
MMP2	GAT GTC GCC CCT AAA ACA GAC
	CAG CCA TAG AAA GTG TTC AGG T
MMP9	GGA CCC GAA GCG GAC ATT G
	GAA GGG ATA CCC GTC TCC GT
IL-1β	TCC AGG ATG AGG ACA TGACAC
	GAA CGT CAC ACA CAC GAGCAG GTT A
TGF-β	TGC TAA TGG TGG ACC GCA A
	CAC TGC TTC CCG AAT GTC TGA
GAPDH	GGT GAA GGT CGG TGT GAA ACG
	CTC GCT CCT GGA AGA TGG TG